A

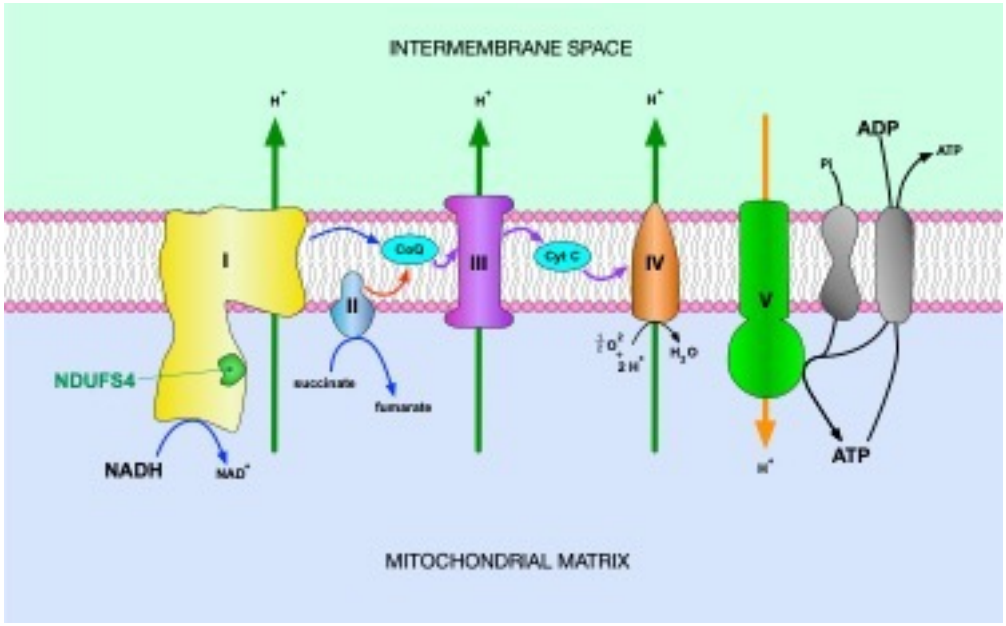
INTERMEMBRANE SPACE
H+
H+
H+
ADP
ATP
Pi
I
II
III
IV
V
CoQ
Cyt C
NDUFS4
succinate
fumarate
NADH
NAD+
ATP
MITOCHONDRIAL MATRIX

B

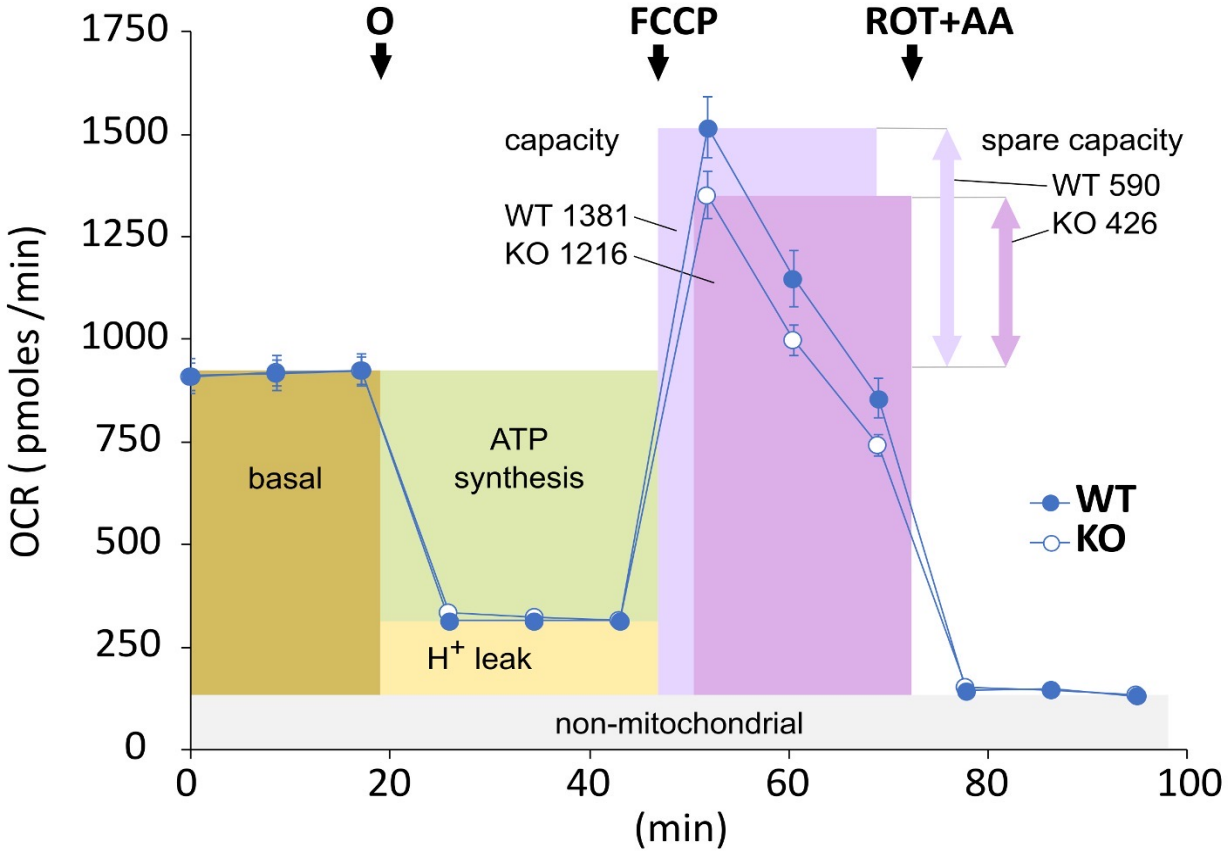
O
FCCP
ROT+AA
1750
1500
1250
1000
750
500
250
0
OCR (pmoles /min)
capacity
spare capacity
WT 590
KO 426
WT 1381
KO 1216
basal
ATP
synthesis
H+ leak
non-mitochondrial
WT
KO
0
20
40
60
80
100
(min)

Figure S1. Baseline Energetics and Synaptic Function in Physiologic Conditions. Related to STAR Methods, Figure 7, Results (A,B) and Discussion (B). A. The mitochondrial electron transport chain and Ndufs4. Complex I receives electrons from NADH and passes them to coenzyme Q (CoQ) which then transfers them to complexes III and IV. Complexes I, III and IV pump hydrogen ions into the mitochondrial intermembrane space to drive Complex V to make ATP. Previous work has shown complex I to be sensitive to the inhibitory effects of isoflurane in both C. elegans and mice. NDUFS4 is an assembly/stabilizing subunit for complex I. **B**. Mitochondrial respiration of primary hippocampal cells measured with a Seahorse flux analyzer. Traces show mean oxygen consumption rates (OCR) (±SEM error bars) for 10 wells of Ndufs4(KO) and wildtype control cells each after 10 days in culture. The medium contained 1.5mM glucose and 10mM pyruvate to sustain respiration. Arrows indicate the time when drugs “O” (oligomycin, complex V inhibitor), “FCCP” (an uncoupler), “ROT+AA” (rotenone (complex I inhibitor) and antimycin A (complex III inhibitor)) were injected. The basal respiration, and the respiration devoted to ATP synthesis of Ndufs4(KO) were indistinguishable from controls, suggesting adequate energy supply of the resting KO cells. Uncoupling with FCCP approximates the respiration capacity. Mean OCR values for capacity and spare capacity are given as numbers. There were no significant differences between genotypes.

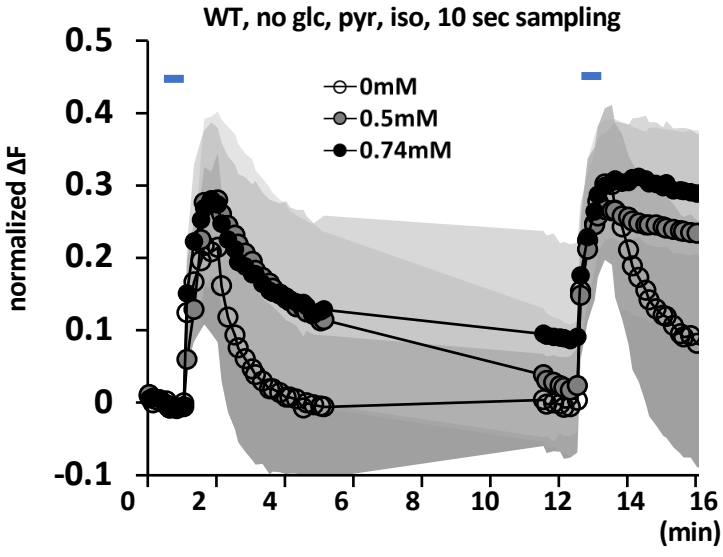
WT, no glc, pyr, iso, 10 sec sampling
normalized ΔF
0mM
0.5mM
0.74mM
(min)

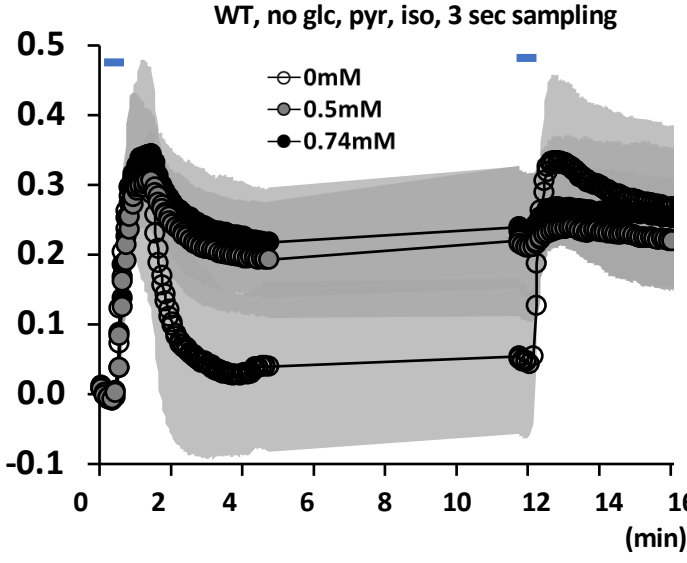
WT, no glc, pyr, iso, 3 sec sampling
0mM
0.5mM
0.74mM
(min)

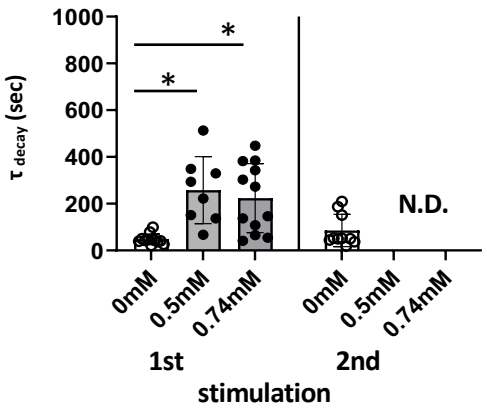
τ decay (sec)
N.D.
0mM
0.5mM
0.74mM
1st
2nd
stimulation

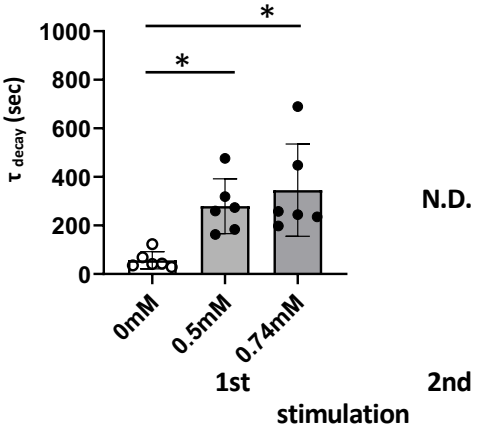
τ decay (sec)
N.D.
0mM
0.5mM
0.74mM
1st
2nd
stimulation

Figure S2. pHluorin Signal with Restricted Glucose at Two Acquisition Rates. Related to Results and Star Methods. Exocytosis and endocytosis following electrical field stimulation of hippocampal cultures with no exogenous glucose, supplemented with pyruvate. **Upper left panel.** Wild type cells electrically stimulated in the absence or presence of isoflurane (0.5mM and 0.74mM) with acquisition rates of 10 second sampling (0.1Hz). These data are a repeat of the protocol shown in Figure 3 but were redone here as a control for the faster acquisition rate of 3 second sampling (0.3Hz)) shown in the Right Panel. *Upper right panel***.** Wild type cells electrically stimulated in the absence or presence of isoflurane (0.5mM and 0.74mM) with acquisition rates of every 3 seconds (0.3Hz). Note the failure in return to baseline of the unexposed sample following the second stimulation. However, as seen in left panel at the lower acquisition rate, there was a failure to return to baseline at both isoflurane concentrations. **Lower left and right panels.** Decay time increased following the first stimulation for both isoflurane concentrations at both acquisition rates. In addition, there was an inability to calculate tau (complete failure of endocytosis) in at both acquisition rates in the presence of isoflurane following the second stimulation. However, since the unexposed culture with a 0.3Hz acquisition rate failed to return to baseline following the second stimulation in the absence of isoflurane, it is not possible to determine the specific effects of isoflurane following the second stimulation.

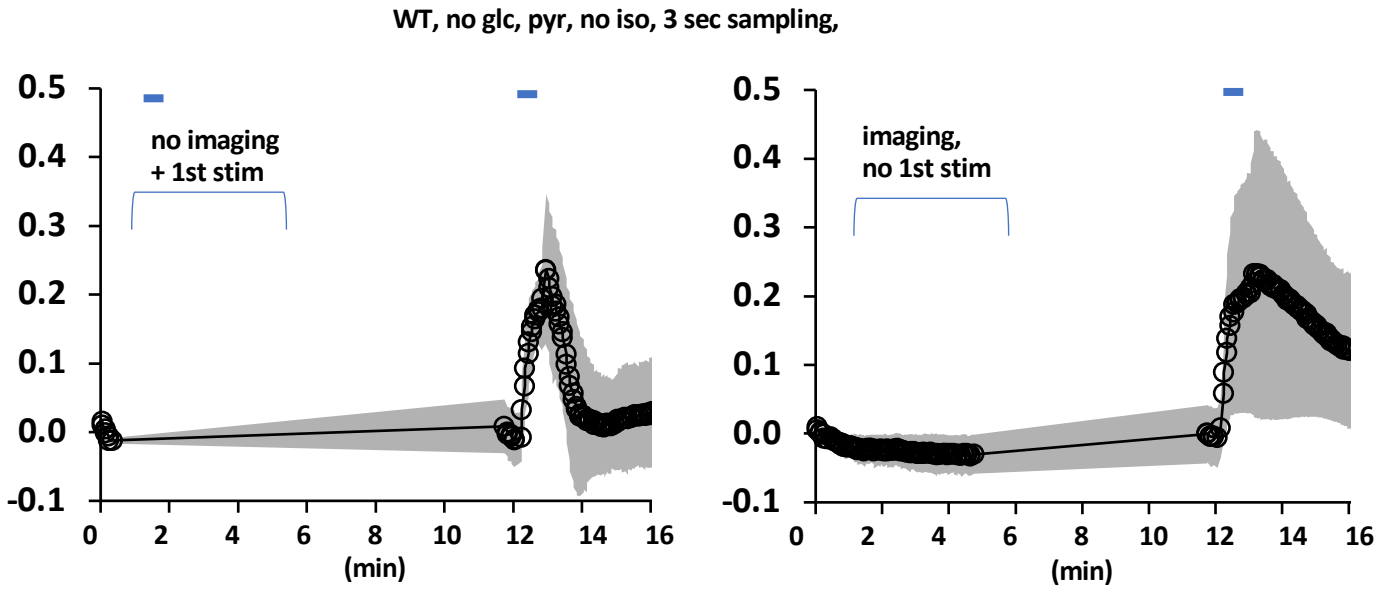
WT, no glc, pyr, no iso, 3 sec sampling,
no imaging
+ 1st stim
imaging,
no 1st stim
0.5
0.4
0.3
0.2
0.1
0.0
-0.1
0
2
4
6
8
10
12
14
16
(min)

Figure S3. The pHluorin signal recovery is dependent specifically on acquisition rate. Related to Results and Star Methods. Left panel. When unexposed cultures were stimulated without fluorescent imaging during the first stimulation, but which were exposed to imaging every 3 seconds during a second stimulation, no defect in the decay time was seen in the first fluorescent exposure following the second electrical stimulation. **Right panel.** When cultures were exposed to the first fluorescent exposure at 0.3Hz, but not electrically stimulated during the first time period, a defect in the decay time was seen in the second fluorescent exposure at 0.3Hz following the electrical stimulation at 12 minutes, indicating that two fluorescent exposures, not electrical stimulation, caused the defect in signal recovery.

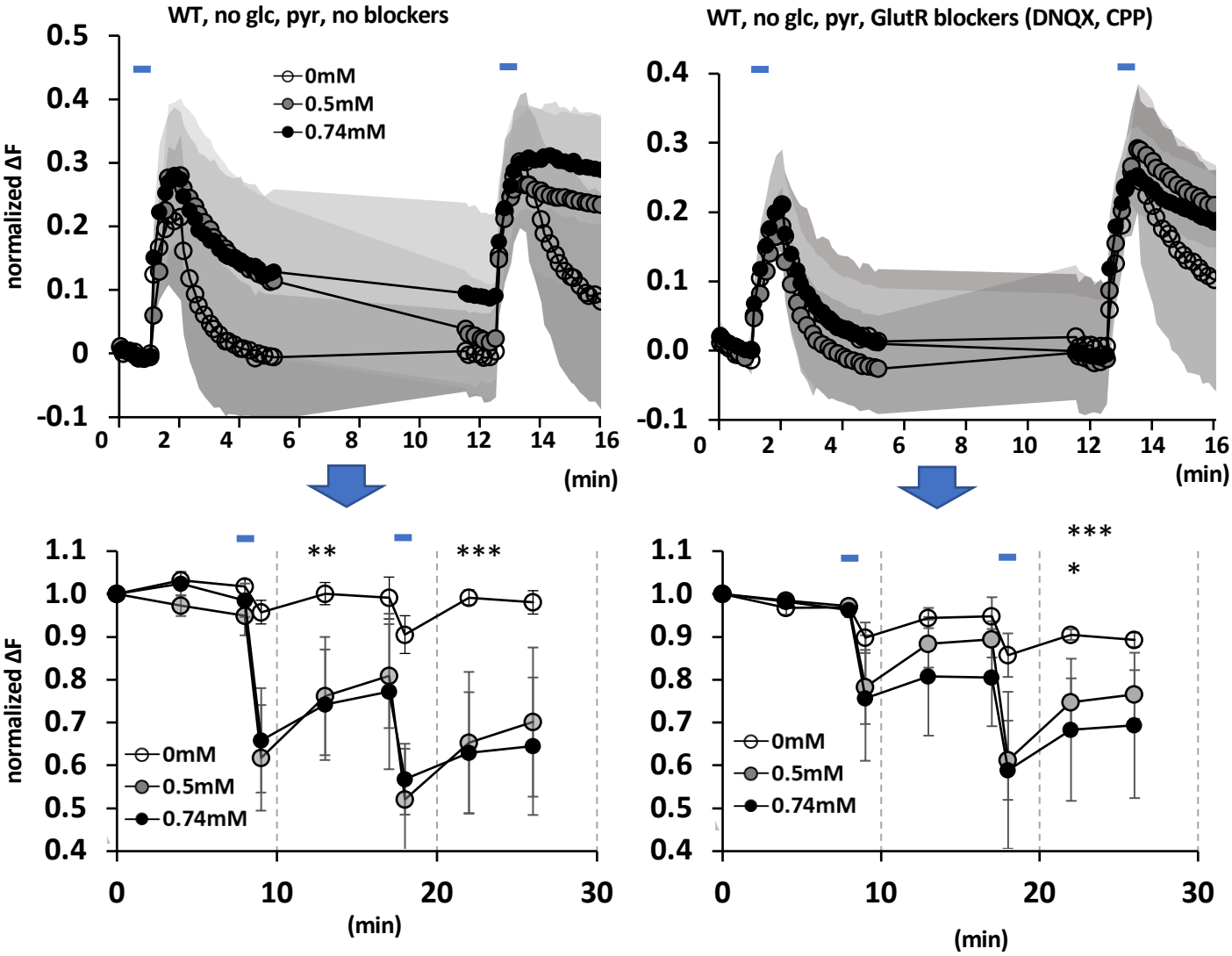
WT, no glc, pyr, no blockers
WT, no glc, pyr, GlutR blockers (DNQX, CPP)
normalized ΔF
0mM
0.5mM
0.74mM
(min)
**
***
*

Figure S4. Synaptic Functioning with Restricted Network Input. Related to Results and Figure 5. Upper Panel. Exocytosis and endocytosis in absence (**left panel**) and presence of (**right panel**) glutamatergic blockade. To decrease stimulation input, glutamatergic receptors were blocked with antagonists, 6,7-dinitroquinoxaline-2,3-dione (10uM) and 3-(2-Carboxypiperazin-4-yl)propyl-1-phosphonic acid (10uM). Wild type cells in 0.5mM or 0.74mM isoflurane in 0mM glucose supplemented with pyruvate. In the presence of isoflurane, endocytosis was markedly defective following the second stimulation in the presence of glutamatergic blockade. Left panels represent wildtype cells in the absence of glutamatergic blockade, right graphs represent wildtype cells in the presence of glutamatergic blockade. **Lower Panels**. ATP levels under similar protocols as in the upper panels. Wild type cells in 0.5mM or 0.74mM isoflurane in 0mM glucose supplemented with pyruvate. In the presence of isoflurane, ATP levels was decreased following the second stimulation in the presence of glutamatergic blockade. Left panels represent wildtype cells in the absence of glutamatergic blockade (as in Figure 3), right graphs represent wildtype cells in the presence of glutamatergic blockade (as in Figure 5C).